Supplementary Figures

Supplementary Figure 1. Additional *in vivo* glucose homeostasis assessment of male and female pSENP1-KO mice on CD.

(A) Fasting insulin; **(B)** fasting glucose, **(C)** body weight, and **(D)** IP insulin tolerance of pSENP1-WT, -HET and -KO male mice on CD (n=6-22 mice). **(E)** Fasting insulin, **(F)** fasting glucose, **(G)** body weight, and **(H)** IP insulin tolerance of pSENP1-WT, -HET and -KO female mice on CD (n=7-17 mice).

AUC - area under the curve. Data are mean ± SEM and were compared with student t test, one-way or two-way ANOVA followed by Bonferroni post-test. Unless stated otherwise, *-$p<0.05$, indicated comparison between pSENP1-WT and -KO.

Supplementary Figure 2. *In vivo* glucose homeostasis assessment of female pSENP1-KO mice following HFD.

(A) OGTT and **(B)** associated plasma insulin responses, **(C)** IP insulin tolerance, **(D)** body weight, **(E)** fasting glucose, and **(F)** fasting insulin of pSENP1-WT, -HET and -KO female mice following HFD (n=9-14 mice).

Supplementary Figure 3. Islet morphometry analysis of female pSENP1-KO mice after HFD.

(A) Representative immunostaining, β-cell mass, islet number, and islet size distribution of female pSENP1-WT (n = 5 mice, 15 sections and 189 islets) and pSENP1-KO (n = 6 mice, 18 sections and 197 islets) following HFD. Insulin (green), glucagon (red), and nuclei (blue).

Scale bar=100 μm. Data are presented as mean ± SEM.

Supplementary Figure 4. Additional *in vivo* glucose homeostasis assessment of βSENP1-KO male mice.

(A) IP insulin tolerance of male βSENP1-WT, -HET, and -KO mice following HFD (n=15, 8, 8 mice). **(B)** Delta area under the curve (ΔAUC) of IP insulin tolerance tests of male βSENP1-WT, -HET, and -KO mice on CD and following HFD (n=6, 6, 6, 15, 8, 8 mice). **(C)** Fasting insulin of male βSENP1-WT, -HET, and -KO mice on CD and following HFD (n=6, 4, 5, 13, 17, 14). **(D)** fasting glucose (n=15-22 mice) levels and **(E)** Body weight (n=18-23 mice) in male βSENP1-WT and -KO mice on CD and following HFD.

Data are presented as mean ± SEM. AUC - area under the curve. Data are mean ± SEM and were compared with student t test, one-way or two-way ANOVA followed by Bonferroni post-test. Unless stated otherwise, *-$p<0.05$, indicated comparison between βSENP1-WT and -KO.

Supplementary Figure 5. *In vivo* glucose homeostasis assessment of βSENP1-KO female mice.

(A) Fasting insulin (n=6, 8, 4, 13, 16, 14 mice), **(B)** fasting glucose (n=21, 22, 20, 21, 21, 22), and **(C)** body weights (n=30, 23, 25, 20, 22, 22) of female βSENP1-WT, -HET, and -KO mice on CD and following HFD. **(D)** OGTT (n=11, 12, 12 mice), **(E)** IPGTT (n=10, 11, 9 mice), and **(F)** IP insulin tolerance (n=6, 9, 8) of female βSENP1-WT, -HET and -KO mice on CD. **(G)** OGTT (n=11, 13, 11 mice) and **(H)** associated plasma insulin response (n=7, 7, 8 mice) of female βSENP1-WT, -HET, and -KO mice following HFD. **(I)** IPGTT (n=8, 9, 10 mice), and **(J)** associated plasma insulin response (n=6, 9, 6 mice) of female βSENP1-WT, -HET, and -KO mice following HFD. **(K)** IP insulin tolerance (n=11, 11, 12 mice) of female βSENP1-WT, -HET and -KO female mice following HFD and associated ΔAUC for CD and HFD. Data are presented as mean ± SEM.

AUC - area under the curve. Data are mean ± SEM and were compared with student t test, one-way or two-way ANOVA followed by Bonferroni post-test. Unless stated otherwise, *-$p<0.05$, **-$p<0.01$, indicated comparison between βSENP1-WT and -KO.

Supplementary Figure 6. Islet mass analysis of male and female βSENP1-KO mice after CD and HFD feeding.

(A) Representative immunostaining images, and **(B)** β-cell mass, islet number, and islet size distribution of male βSENP1-WT mice on CD (n = 3 mice, 9 sections and 162 islets), male βSENP1-KO mice on CD (n = 4 mice, 13 sections and 139 islets), male βSENP1-WT mice following HFD (n = 6 mice,18 sections and 340 islets) and βSENP1-KO mice following HFD (n = 3 mice, 9 sections and 200 islets). **(C)** Representative immunostaining image, **(D)** islet mass, islet number, islet size accumulative frequency of female βSENP1-WT mice on CD (n = 5 mice, 14 sections and 146 islets), βSENP1-KO mice on CD (n = 4 mice, 12 sections and 101 islets), βSENP1-WT mice following HFD (n = 5 mice,15 sections and 155 islets) and βSENP1-KO mice following HFD (n = 4 mice, 11 sections and 141 islets). Insulin (green), glucagon (red), and nuclei (blue).

Scale bar=100 μm. Data are mean ± SEM and were compared with one-way or two-way ANOVA followed by Bonferroni post-test. *-$p< 0.05$, **-$p<0.01$, ***-$p<0.001$ indicated comparison between HFD and CD.

Supplementary Figure 7. Calcium response and nutrient-stimulated insulin secretion βSENP1-KO mice after HFD feeding.

(A) Average voltage-dependent Ca^{2+} currents of β-cell elicited by a single 500 ms membrane depolarization from -70 mV to 0 mM at 5mM glucose or with Ex4 or GIP (n=50, 55, 56, 47, 51, 46 cells from 5 mice per group). cAMP was omitted in pipette solution. **(B)** Insulin secretion to glucose and oleate (n=3 pairs of mice after HFD). **(C)** Insulin secretion to glucose and amino acids (n=5 pairs of mice after CD). **(D-E)** Calcium response, baseline, and amplitude in response to glucose with Ex4 (D - n=4 pairs of mice, 73 and 88 cells) or GIP (E – n= 4 pairs of mice, 68 and 74 cells).

AUC - area under the curve. Data are mean ± SEM and were compared with student t test, one-way or two-way ANOVA followed by Bonferroni post-test. Unless stated otherwise, *-$p<0.05$, **-$p<0.01$, ***-$p<0.001$ indicated comparison between βSENP1-WT and -KO.

Supplementary Figure 8. FRET-based imaging of cAMP in whole islets.

Islets were infected with adenovirus expressing the cAMP biosensor (Epac-SH187, Kd = 4 μM) under control of the rat insulin promoter. **(A)** Representative images of 1,1-dioctadecyl-3,3,3,3-tetramethylindotricarbocyanine iodide (DiR) loaded islets, and R470/535 emission ratios at time=0 and time=25 minutes. **(B)** Normalized single wavelength emission of the probe at 470 and 535 nm is shown, with expected increases (470 nm) and decreases (535 nm) of emission in response to Ex4 (10 nM; n=4 pairs of mice, 68 and 74 islets) or GIP (100 nM; n=4 pairs of mice, 73 and 88 islets).

Supplementary table 1

Primer Name	Accession	5'-3' primer sequence	Amplicon length (bp)
SENP1 Preamplification	NM_144851.5	FW- CTACATGAACATGCTAATGGAACG RV-AAGAGGATCCTGCAGGCC	284
SENP1 Nested qPCR	NM_144851.5	FW-AAGAGAAGGGGTTTCCAAGTG RV-CCTCGTTGTTTATTCCACCCATAG	228
Cyclophilin A Preamplification	NM_008907.2	FW-TGCAGACAAAGTTCCAAAGACAGCAG RV-TGGTGATCTTCTTGCTGGTCTTGC	398
Cyclophilin A Nested qPCR	NM_008907.2	FW-TGGCTATAAGGGTTCCTCCTTTCACAG RV-GCCAGGACCTGTATGCTTTAGGATG	151

Supplementary Figure 1

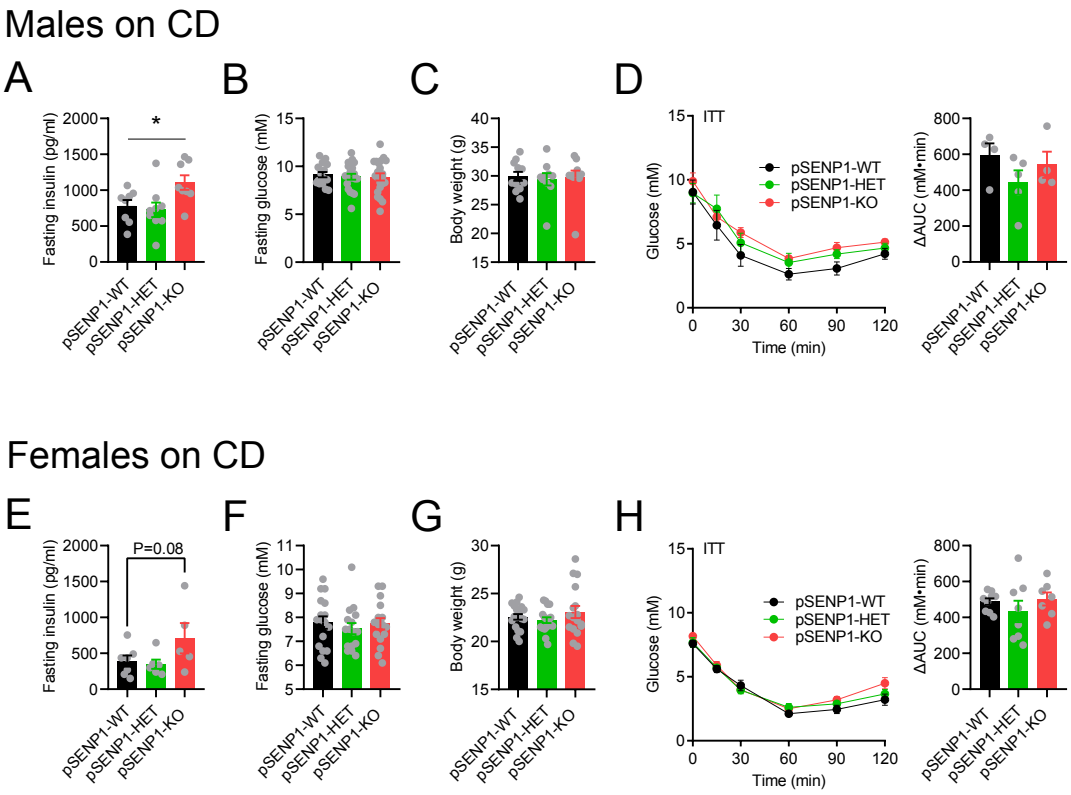

Supplementary Figure 2

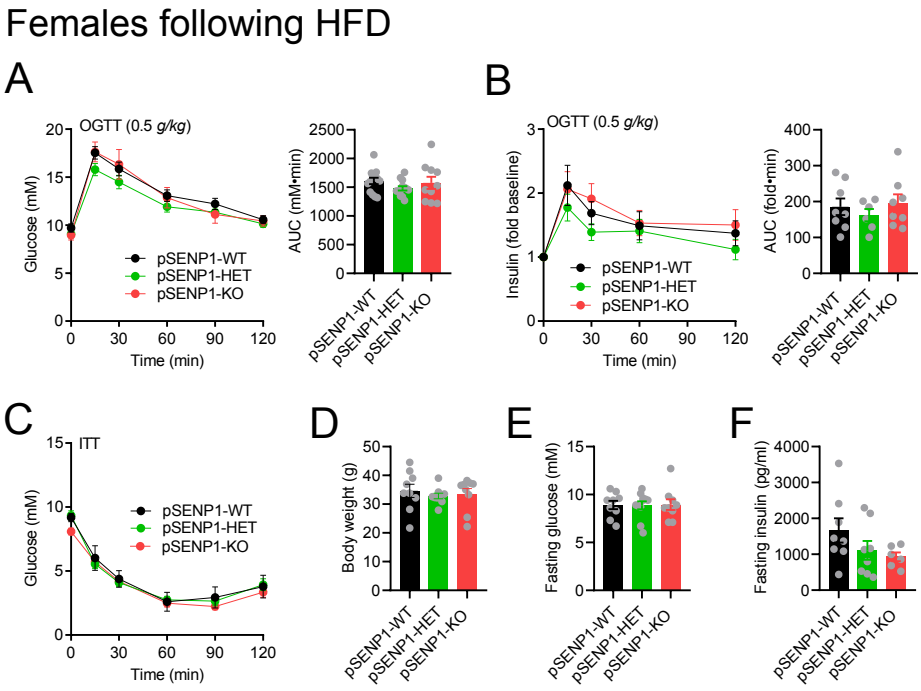

Supplementary Figure 3

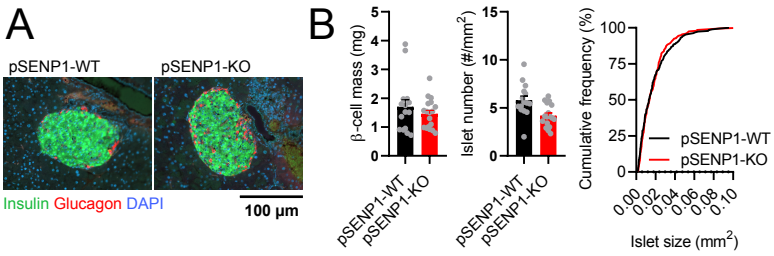

Supplementary Figure 4

Male mice

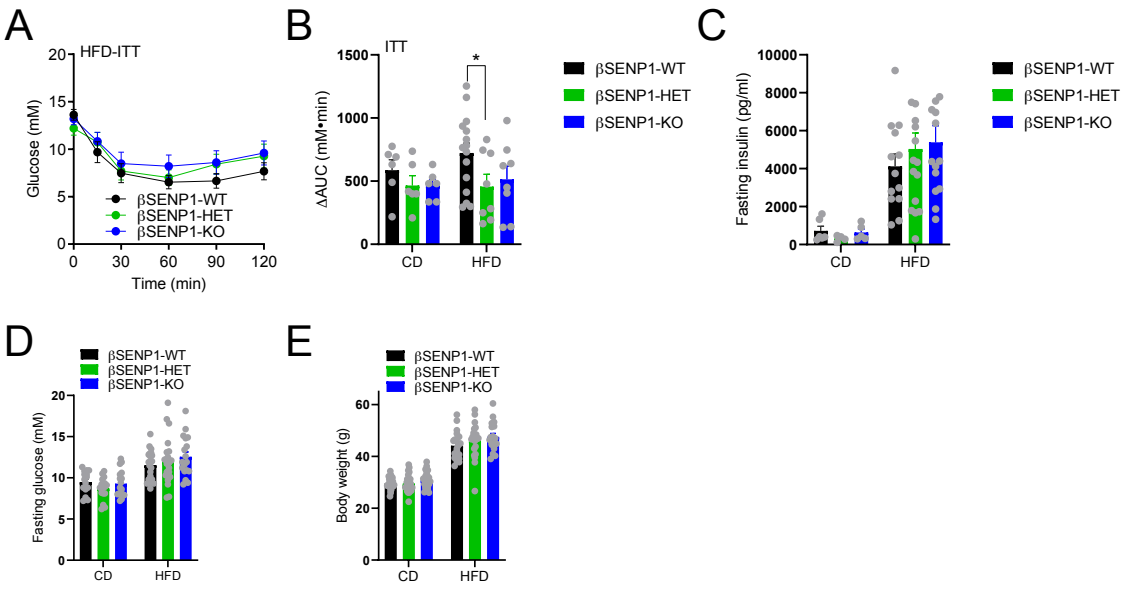

Supplementary Figure 5

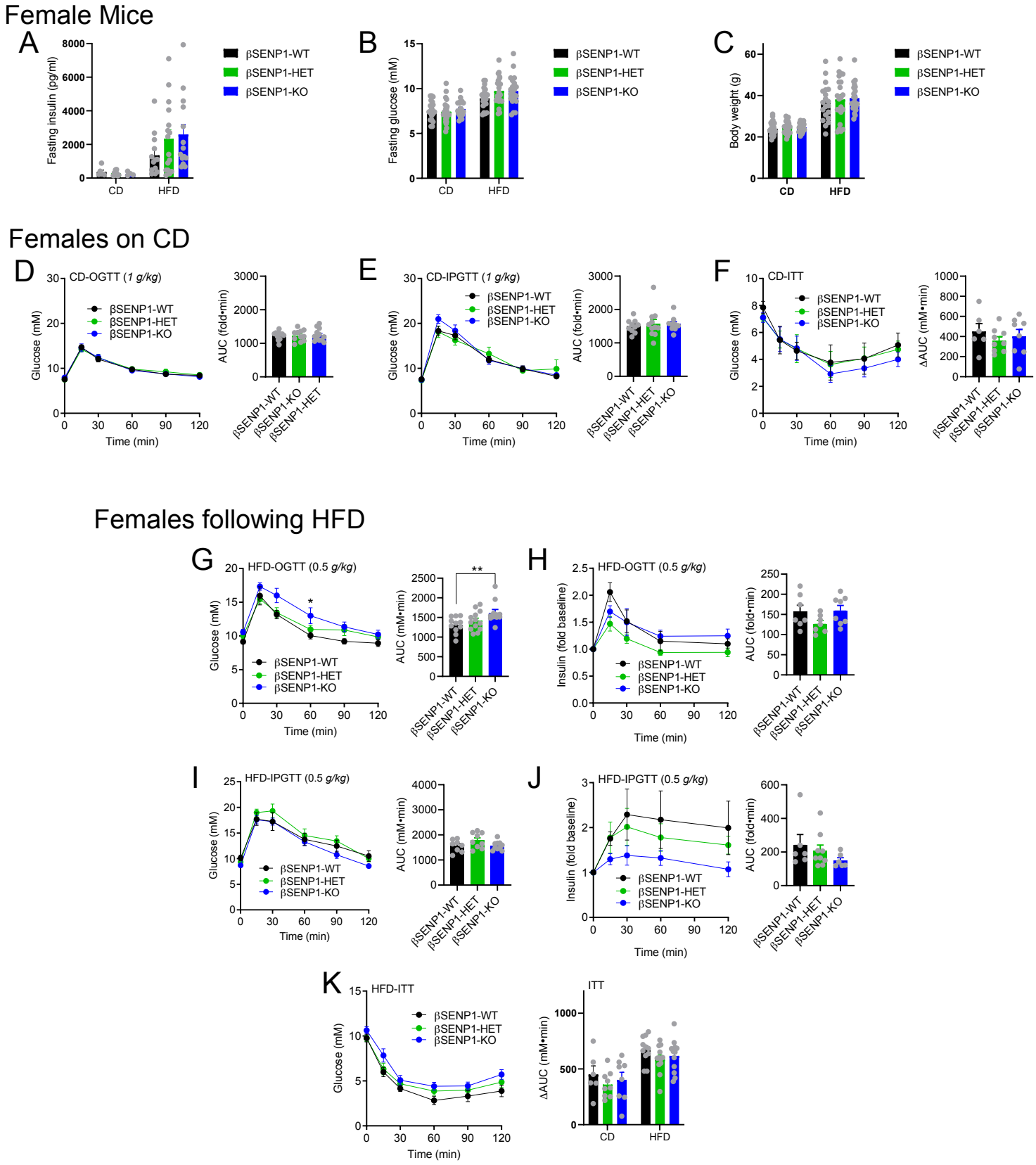

Supplementary Figure 6

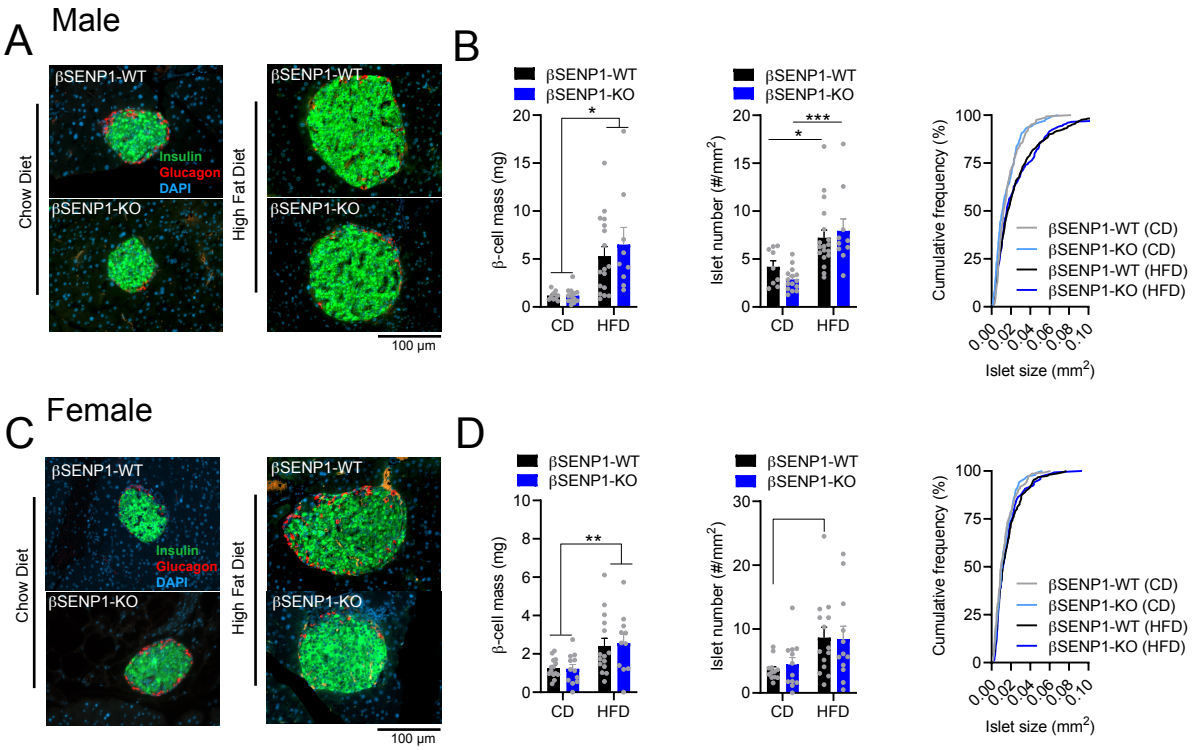

Supplementary Figure 7

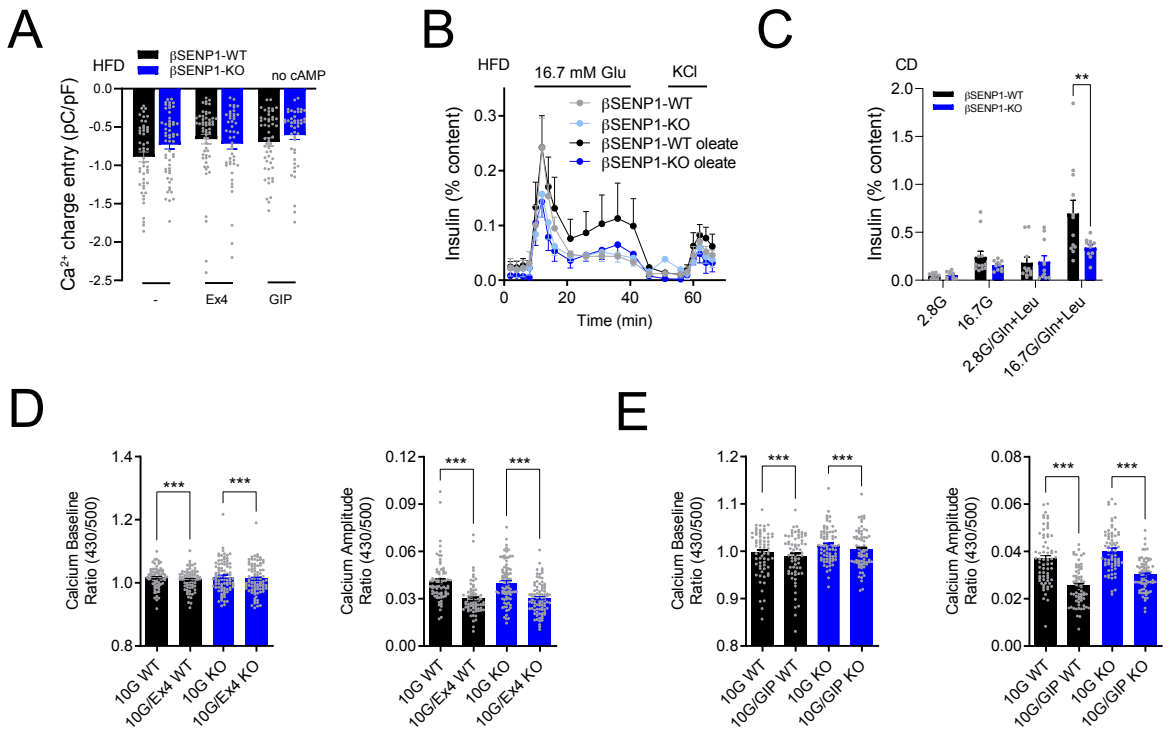

Supplementary Figure 8